Available online at www.sciencedirect.com
SCIENCE DIRECT®
ELSEVIER
Computers and Mathematics with Applications 47 (2004) 593–609
An International Journal
computers & mathematics with applications
www.elsevier.com/locate/camwa

The Numerical Solution of Exterior Neumann Problem for Helmholtz's Equation via Modified Green's Functions Approach

TZU-CHU LIN
Department of Mathematics, University of Wisconsin-Milwaukee
Milwaukee, WI 53201, U.S.A.

Y. WARNAPALA-YEHIYA
Department of Mathematics, Roger Williams University
Bristol, RI 02809-2921, U.S.A.

(Received January 2003; accepted February 2003)

Abstract—In the 1970s, modified Green's function approach for solving the Helmholtz equation was proposed by Jones and Ursell and in the 1980s was clarified by Kleinman, Roach and Kress. To this date there are no numerical results available for this approach. In this paper, a global Galerkin method is used to numerically solve the exterior Neumann problem for the Helmholtz equation in three dimensions based on Jones' modified integral equation approach. Jones approach directly leads to an integral equation which only involves weakly singular operators, thus is a good alternative for solving the exterior Neumann problem. Theoretical and computational details of the method are presented.

Keywords—Helmholtz equation, Neumann problem.

1. INTRODUCTION

Many scattering and radiation problems are concerned with finding solutions of Helmholtz's equation,

$$\Delta u + k^2 u = 0, \qquad \operatorname{Im} k \geq 0,$$

in an exterior domain. Finite-element methods and finite-difference methods are the most popular numerical methods for solving elliptic partial-differential equations. But for Helmholtz's equation, there is a fundamental difficulty in using these methods. The difficulty is that the region of interest is of infinite extent and any solution must satisfy the radiation condition at infinity. Integral equation methods avoid these difficulties.

The integral equation is solved only on the boundary, and it satisfies the radiation condition automatically. Therefore, the integral equation approach is widely recognized as the best approach for solving exterior problems for Helmholtz's equation. Let the solutions of the exterior Neumann problem be expressed as a single layer potential, which is the classic way to solve the

We would like to thank K. Atkinson of University of Iowa for giving us a copy of his computer program for the Laplace's equation for the Neumann problem.

0898-1221/04/$ - see front matter Typeset by AMS-TEX
doi: 10.1016/S0898-1221(04)00049-5

Laplace's equation. If this method is used for Helmholtz's equation, it will break down for certain values of k, namely when k is an eigenvalue of the interior Dirichlet problem.

A second approach uses the Helmholtz's representation formula. If we use the Helmholtz's formula, the uniqueness of the solution of the integral equation is again in question. Beginning in the 1960s, many researches tried to find an integral equation approach which holds for all k.

Much of the work done uses a finite-element framework in solving the integral equation. The resulting numerical methods are quite flexible for a large variety of surfaces, but they often converge slowly. They also lead to relatively large linear systems which must be solved by iteration.

The following representations for the integral equation for the exterior Neumann problem are known: the CHIEF (combined Helmholtz integral equation formulation) introduced by Schenk [1], the integral equation approach by Burton and Miller [2], and the modified integral equation formulation introduced by Jones [3]. CHIEF involves choosing suitable interior points away from the wave numbers and leads to weakly singular operators. Burton and Miller's integral equation approach for solving the exterior Neumann problem for Helmholtz equation leads to a hypersingular integral equation, which needs a regularization technique that leads to several composite weak singular operators. In the last two decades, these formulations were widely used and discussed in Acoustics (see Journal of Acoustic Society of America).

To overcome the nonuniqueness problem arising in integral equations for the exterior boundary-value problems for the Helmholtz's equation, Jones [3] suggested adding a series of outgoing waves to the free-space fundamental solution. To this date, there are no numerical results available for the Jones method. Jones approach only leads to a weak singular integral equation, thus is a viable alternative for solving the exterior Neumann problem. In this paper, we apply the same Galerkin method used by Lin [4], for solving the exterior Neumann problem of the Helmholtz equation based on Jones integral equation approach. We restrict ourselves to regions with smooth boundaries. When the surface and the boundary function are sufficiently smooth, our method will lead to quite small linear systems and will converge quickly.

We begin with definitions, properties, and an introduction to the radiating waves. Smoothness results of the integral operator are summarized in Section 3. The spherical harmonics which are the basis functions of our method are defined in Section 4, and the related approximation results are stated there. The Galerkin method is defined in Section 5, and rates of convergence are derived by using smoothness results. The practical implementation of the numerical method is covered in Section 6. Numerical examples are given in Section 7. The accuracy of the Galerkin coefficients on the unit sphere is given in Section 8.

2. DEFINITIONS AND PRELIMINARY RESULTS

Let S be a closed bounded surface in $\Re^3$ and assume it belongs to the class of C^2. Let D_-, D_+, denote the interior and exterior of S, respectively. The exterior Neumann problem for Helmholtz's equation is

$$\begin{aligned} \Delta u(A) + k^2 u(A) = 0, \quad A = (x,y,z) \in D_+, \qquad \operatorname{Im} k \geq 0, \\ \frac{\partial u(p)}{\partial \nu_p} = f(p), \qquad p \in S, \end{aligned} \tag{2.1}$$

with f a given function and u satisfying the Sommerfeld radiation condition

$$u = O\left(\frac{1}{r}\right), \quad \left(\frac{\partial}{\partial r} - ik\right) u = o\left(\frac{1}{r}\right), \qquad \text{as } r = |A| \longrightarrow \infty. \tag{2.2}$$

Before we discuss the integral equation formulation, we introduce the following notation. We call

$$L_k \mu(p) = \int_s \mu(q) \frac{e^{ik|p-q|}}{|p-q|} d\sigma_q, \qquad p \in \Re^3 \tag{2.3}$$

a single layer function, and $\mu(q)$ is called the single layer density function. For simplicity, sometimes we write $L_k\mu$ only. We note that when $k = 0$ this is the single layer potential satisfying the Laplace's equation.

Integral Equation Formulation

The exterior Neumann problem is first reformulated as an integral equation. The solution is represented as a modified single layer potential, based on the modified fundamental solution (see [5]):

$$u(A) = \int_S \mu(q) \left(\frac{e^{ikr_{qA}}}{4\pi r_{qA}} + \chi(A,q) \right) d\sigma_q, \tag{2.4}$$

with $A \in D_+$, where $r_{qA} = |A - q|$.

The series of radiating waves is given by

$$\chi(A,q) = ik \sum_{n=0}^{\infty} \sum_{m=-n}^{n} a_{nm} h_n^{(1)}(k|A|) Y_n^m \left(\frac{A}{|A|} \right) h_n^{(1)}(k|q|) \overline{Y_n^m} \left(\frac{q}{|q|} \right). \tag{2.5}$$

Here $h_n^{(1)}$ denote the spherical Hankel function of the first kind and of order n.

Then $h_n^{(1)} = j_n + iy_n$

$$j_n(z) = \frac{\sqrt{\pi}}{2} \left(\frac{z}{2} \right)^{-1/2} J_{n+1/2}(z), \qquad \text{where } J_{n+1/2}(z) = \sum_{k=0}^{\infty} \frac{(-1)^k (z/2)^{n+1/2+2k}}{k!\Gamma(n+1/2+k+1)},$$

$$y_n(z) = \frac{\sqrt{\pi}}{2} \left(\frac{z}{2} \right)^{-1/2} Y_{n+1/2}(z), \qquad \text{where } Y_{n+1/2}(z) = \frac{J_{n+1/2}\cos(z\pi) - J_{-(n+1/2)}(z)}{\sin(z\pi)},$$

and

$$h_n^{(1)}(z) = \frac{\sqrt{\pi}}{2} \left(\frac{z}{2} \right)^{-1/2} H_{n+1/2}^{(1)}(z).$$

By Y_n^m, $n = -m, \ldots, m$, we denote the linearly independent spherical harmonics of order m given by $Y_n^m(\phi,\theta) = ((1/2\pi)(m+1/2)((m-n)!/(m+n)!))^{1/2} p_n^m(\cos\theta) e^{im\phi}$ where p_n^m denote the associated Legendre polynomials (these will be discussed later more extensively).

The series χ is a solution to the Helmholtz equation satisfying the Sommerfeld radiation condition for $|x|, |y| > R$, when $B = \{x : |x| \le R\}$ is contained in D, a domain containing the origin.

As in [6], we assume D_- to be a domain containing the origin and we choose a ball B of radius R and center at the origin such that $\bar{B} \subset D_-$. On the coefficients a_{nm} we impose the condition that the series $\chi(p,q)$ is uniformly convergent in p and in q in any region $|p|, |q| \ge R+\epsilon$, $\epsilon > 0$, and that the series can be two times differentiated term by term with respect to any of the variables p, q with the resulting series being uniformly convergent. By letting A tend to a point $p \in S$, we obtain an integral equation

$$2\pi\mu(p) + \int_S \mu(q) \frac{\partial \Psi(p,q)}{\partial \nu_p} d\sigma_q = -4\pi f(p), \qquad p \in S, \tag{2.6}$$

where $\Psi(p,q) = -e^{ikr_{qp}}/r_{qp} - 4\pi\chi(p,q)$.

We denote the above integral equation by

$$2\pi\mu + K\mu = -4\pi f, \tag{2.7}$$

where $K\mu(p) = \int_S \mu(q) \frac{\partial}{\partial \nu_p} (-e^{ikr_{qp}}/r_{qp} - 4\pi\chi(p,q))\, d\sigma_q$.

By the assumptions on the series $\chi(p,q)$ the kernel $\frac{\partial \chi(p,q)}{\partial \nu_p}$ is continuous on $S \times S$, and hence, K is compact from $C(S)$ to $C(S)$ and from $L^2(S)$ to $L^2(S)$.

The following existence and uniqueness theorem is known.

THEOREM 2.1. *(See [6].) The modified single layer integral equation (2.6) for the exterior Neumann problem is uniquely solvable for all positive wave numbers $k > 0$ provided that either $|2a_{nm} + 1| < 1$, for all $n = 0, 1, 2, \ldots$, $m = -n, \ldots, n$ or $|2a_{nm} + 1| > 1$, for all $n = 0, 1, 2, \ldots, m = -n, \ldots, n$.*

Kleinman and Roach [7] proposed some explicit choices for the coefficient a_{nm} which optimize the modification with respect to various criteria. In particular, one optimality condition that might be employed is to minimize the norm of the integral operator K. In the case where S is a sphere, Kleinman and Roach [7] gave a coefficient choice which satisfies the condition in Theorem 2.1. It is

$$a_{nm} = -\frac{j_n'(kR)}{h_n^{(1)'}(kR)}. \tag{2.8}$$

In [8], an explicit form of the coefficient a_{nm} minimizing the upper bound on the spectral radius is given. If B is a sphere of radius R with center at the origin, then the optimal coefficient for the Neumann problem was given by

$$a_{nm} = -\frac{1}{2}\left(\frac{j_n(kR)}{h_n^{(1)}(kR)} + \frac{j_n'(kR)}{h_n^{(1)'}(kR)}\right), \qquad \text{for } n = 0, 1, 2, \ldots, \quad \text{and} \quad m = -n, \ldots, n. \tag{2.9}$$

The coefficient that they used for the perturbation of the sphere is the following:

$$a_{nm} = -0.5\left(\frac{j_n(kR)}{h_n^{(1)}(kR)} + \frac{j_n'(kR)}{h_n^{(1)'}(kR)}) + O(\epsilon)\right) \tag{2.10}$$

(also see [8]). We also did some numerical experiments for the special ellipsoid, the ellipsoid of revolution around the z axis.

3. SMOOTHNESS OF THE INTEGRAL OPERATOR K

Smoothness results of the double layer operator was proven by Lin [4,9]. We know that the series χ can be twice differentiated term by term with respect to any of the variables and that the resulting series is uniformly convergent. So the second derivative of the series is continuous on $\Re^3 \backslash B$, where $B = \{x : |x| \leq R\}$. Furthermore, the series χ is a solution to the Helmholtz equation satisfying the Sommerfeld radiation condition for $|x|, |y| > R$, when $B = \{x : |x| \leq R\}$ is contained in D.

By Theorem 3.5 of [6], any two times continuously differentiable solution to the Helmholtz's equation is analytic, and analytic functions are infinitely differentiable. So the series $\chi(p, q)$ is infinitely differentiable with respect to any of the variables p, q. Furthermore, it is easy to see that if μ is bounded and integrable and $S \in C^l$, then $\int_S \chi(p, q)\ \mu(q) d\sigma_q \in C^l(S)$ and $\frac{\partial}{\partial \nu_p} \int_S \chi(p, q)\mu(q)\, d\sigma_q \in C^l(S)$. Using the same proof as in [9], we can prove the following for the normal derivative of $L_k\mu$ (see (2.3)), denoted by $L_k'\mu$. $\mu \in C(S)$ and $S \in C^{1,\lambda}$ implies

$$L_k'\mu \in C^{0,\lambda'}(S), \qquad \text{with } \lambda' = \begin{cases} \lambda, & \text{if } 0 < \lambda < 1, \\ \text{arbitrary in } 0 < \lambda' < 1, & \text{if } \lambda = 1, \end{cases} \tag{3.1}$$

$\mu \in C^{l,\lambda}(S)$ and $S \in C^{l+2,\lambda}$ implies

$$L_k'\mu \in C^{l+1,\lambda'}(S), \qquad \text{with } 0 < \lambda' < \lambda \text{ arbitrary}, \ l \geq 0. \tag{3.2}$$

Now combining with the smoothness result of $L_k'\mu$, we can obtain the following results. $\mu \in C(S)$ and $S \in C^{1,\lambda}$ implies

$$K\mu \in C^{0,\lambda'}(S), \qquad \text{with } \lambda' = \begin{cases} \lambda, & \text{if } 0 < \lambda < 1, \\ \text{arbitrary in } 0 < \lambda' < 1, & \text{if } \lambda = 1. \end{cases} \tag{3.3}$$

If $f \in C^{0,\lambda}(S), S \in C^2$ and $2\pi\mu + K\mu = -4\pi f$, then

$$\mu \in C^{0,\lambda'}(S), \qquad \text{with } \lambda' \text{ chosen as in (3.3).} \tag{3.4}$$

If f and S have greater smoothness, then so does μ. Corresponding to (3.3)

$$\mu \in C^{l,\lambda}(S) \text{ and } S \in C^{l+2,\lambda} \text{ implies } K\mu \in C^{l+1,\lambda'}(S), \qquad \text{with } 0<\lambda'<\lambda \text{ arbitrary, } l \geq 0. \tag{3.5}$$

Corresponding to (3.4),

$$f \in C^{l,\lambda}(S) \text{ and } S \in C^{l+1,\lambda}(l \geq 1) \text{ implies } \mu \in C^{l,\lambda'}(S), \qquad \text{where } 0 < \lambda' < \lambda. \tag{3.6}$$

REMARK. The restriction $l \geq 1$ in (3.6) only arises from Theorem 3.1 where $S \in C^2$.

4. SPHERICAL HARMONICS AND APPROXIMATION THEORY

Let $U = \{(x, y, z) : x^2 + y^2 + z^2 = 1\}$ be the unit sphere in $\Re^3$. If the homogeneous harmonic polynomials of degree n in $\Re^3$ are restricted to U, their restrictions are called the spherical harmonics of degree n. If any other polynomial is restricted to U, then its restriction is called a spherical polynomial. Now, we introduce the standard basis for the spherical harmonics, which are orthogonal in $L^2(U)$. Let $p_n(u)$ and $p_n^m(u)$ denote the Legendre polynomials and associated Legendre functions on $[-1, 1]$,

$$n \geq 0, \qquad 1 \leq m \leq n, \qquad \text{(see [10])}$$

$$p_n(u) = \frac{1}{2^n n!} \frac{d^n \left(u^2-1\right)^n}{du^n} \qquad \text{and} \qquad p_n^m(u) = \frac{1}{2^n n!} \left(1-u^2\right)^{m/2} \frac{d^{m+n} \left(u^2-1\right)^n}{dt^{m+n}}$$

$$(-n \leq m \leq n).$$

If μ is defined on U, we sometimes write $\mu(\phi, \theta)$ instead of $\mu(x, y, z)$. If μ is a spherical polynomial of degree N, then

$$\mu(\phi, \theta) = \sum_{n=0}^{N} \left\{ A_n p_n(\cos\theta) + \sum_{m=1}^{n} \left(A_n^m \cos(m\phi) + B_n^m \sin(m\phi)\right) p_n^m(\cos\theta) \right\}, \tag{4.1}$$

where

$$\begin{aligned} A_n &= \frac{2n+1}{4\pi} \int_0^{2\pi} \int_0^{\pi} \mu(\phi, \theta)\, p_n(\cos\theta) \sin\theta \, d\theta \, d\phi, \\ \begin{bmatrix} A_n^m \\ B_n^m \end{bmatrix} &= \frac{2n+1}{2\pi} \frac{(n-m)!}{(n+m)!} \int_0^{2\pi} \int_0^{\pi} \mu(\phi, \theta) \begin{bmatrix} \cos m\phi \\ \sin m\phi \end{bmatrix} p_n^m(\cos\theta) \sin\theta \, d\theta \, d\phi. \end{aligned} \tag{4.2}$$

The basis functions

$$p_n(\cos\theta), \quad p_n^m(\cos\theta)\cos(m\phi), \quad p_n^m(\cos\theta)\sin(m\phi), \qquad 1 \leq m \leq n, \tag{4.3}$$

are spherical harmonics of degree n. For $0 \leq n \leq N$, the total number of basis functions is $d(N) = (N+1)^2$. Now, we summarize the following approximation results from [11] (or see [12]). If $\mu \in C^{l,\lambda}(u)$, then there is a sequence of spherical polynomials T_N of degree $\leq N$ for which $\|\mu - T_N\|_\infty \leq C/N^{l+\lambda}$, $N \geq 1$. The spherical polynomials are dense in both $C(U)$ and $L^2(U)$. The expansion of $\mu \in L^2(U)$ in terms of the above basis functions is called the Laplace series. It is given by (4.1), (4.1) with $N = \infty$, and (4.2). Let $P_N\mu$ denote the partial sum of the Laplace series of μ restricted to terms of degree $\leq N$. On $L^2(U)$, P_N is an orthogonal projection operator and $\|P_N\| = 1$. On $C(U)$,

$$\|P_N\| = \left(\sqrt{\frac{8}{\pi}} + \delta_N\right) \sqrt{N}, \qquad \text{with } \delta_N \to 0. \tag{4.4}$$

If $\mu \in C^{l,\lambda}(U)$, then $\|\mu - P_N\mu\|_\infty \leq C_1/N^{l+\lambda-1/2}$.

5. THE GALERKIN METHOD

We change the variable of integration in (2.6), converting it to a new integral equation defined on U. The Galerkin method is applied to this new equation, using spherical polynomials to define the approximating subspaces. We shall suppose that the surface S is such that there is a differentiable mapping $m : U \to_{\text{onto}}^{1-1} S$, a mapping for which the following properties are satisfied.

$$f \in C^{l,\lambda}(S) \quad \text{and} \quad S \in C^{l+1,\lambda}\left(S \in C^2, \text{ for } l = 0\right), \qquad \text{implies } \hat{f} \in C^{l,\lambda}(U), \tag{5.1}$$

where

$$\hat{f}(q) \equiv f(m(q)), \qquad q \in U. \tag{5.2}$$

All of our numerical examples have been for regions D starlike with respect to the origin; but the numerical method is not restricted to such regions. For starlike regions, we assume that a general point of S, $p = m(q)$ is given by

$$p = R(q) \cdot (\xi, \eta, \zeta), \qquad q = (\xi, \eta, \zeta) \in U, \tag{5.3}$$

where the function R is a continuous positive function on U. If $R \in C^{l+1,\lambda}(U)$, then (5.1) is satisfied. Change the variable of integration on (2.6) to obtain the new equation over U,

$$2\pi\hat{\mu} + \hat{K}\hat{\mu} = -4\pi\hat{f}, \qquad \hat{f} \in C(U). \tag{5.4}$$

The notation "$\hat{}$" will denote the change of variable from S to U, as in (5.2).

The inverse operator $(-2\pi + \hat{K})^{-1}$ exists and is bounded on $C(U)$ and $L^2(U)$.

Let $X = L^2(U)$, $\alpha = -2\pi$, and let approximating subspace of spherical polynomials of degree $\leq N$ be denoted by X_N. The dimension of X_N is $d_N = (N+1)^2$, and we let $\{h_1, \ldots, h_d\}$ denote the basis of spherical harmonics given in (4.3).

Galerkin's method for solving (5.4) is given by

$$\left(2\pi + P_N\hat{K}\right)\hat{\mu}_N = -4\pi P_N\hat{f}.$$

The solution is given by

$$\begin{aligned} \hat{\mu}_N &= \sum_{j=1}^{d} \alpha_j h_j, \\ 2\pi\alpha_i(h_i, h_i) + \sum_{j=1}^{d} \alpha_j \left(\hat{K}h_j, h_i\right) &= -4\pi\left(\hat{f}, h_i\right), \qquad i = 1, \ldots, d. \end{aligned} \tag{5.5}$$

The convergence of μ_N to μ in $L^2(S)$ is straightforward. We know $P_N\hat{\mu} \to \hat{\mu}$, for all $\hat{\mu} \in L^2(U)$, from the discussion in Section 4. From standard results it follows that $\|\hat{K} - P_N\hat{K}\| \to 0$. The desired convergence then follows from [13]. Using the smoothness results of the integral operator K from Section 3, and following the same proof as in [11], we can prove Theorem 5.1 and Theorem 5.2.

THEOREM 5.1. *Assume that $f \in C^{l,\lambda}(S), S \in C^{l+1,\lambda}$ ($S \in C^2$ for $l = 0$) and that the mapping m satisfies (4.1) for some $l \geq 0$. Then, for all sufficiently large N, the inverses $(2\pi + P_N\hat{K})^{-1}$ exist and are uniformly bounded and $\|\mu - \mu_N\| \leq c/N^{l+\lambda'}$ where $0 < \lambda' < \lambda$ is arbitrary. The constant c depends on l, μ, and λ'.*

CONVERGENCE IN $C(U)$. To prove uniform convergence of $\hat{\mu}_N$ to $\hat{\mu}$ is slightly more difficult. The main problem is that there are $\hat{\mu}$ in $C(U)$ for which $P_N\hat{\mu}$ does not converge to $\hat{\mu}$. Convergence for all $\hat{\mu}$ would imply uniform boundedness of $\|P_N\|$, contradicting (4.4).

THEOREM 5.2. *Assume that $S \in C^2$ and that m satisfies (5.3) with $l = 0$. Then considering $\hat{K}$ as an operator on $C(U)$,*

$$\left\| \hat{K} - P_N \hat{K} \right\| \to 0, \qquad \text{as } N \to \infty. \tag{5.6}$$

This implies the existence and uniform boundedness on $C(U)$ of $(2\pi + P_N\hat{K})^{-1}$, for all sufficiently large N. Let $(2\pi + \hat{K})\hat{\mu} = -4\pi\hat{f}$ and $(2\pi + P_N\hat{K})\hat{\mu}_N = -4\pi P_N\hat{f}$. If $f \in C^{0,\lambda}(S)$, $\lambda > 1/2$, then $\hat{\mu_N}$ converges uniformly to $\hat{\mu}$. Moreover, if $S \in C^{l+1,\lambda}$ ($S \in C^2$, for $l = 0$) and $f \in C^{l,\lambda}(S)$, $l + \lambda > 1/2$, then $\|\mu - \mu_N\|_\infty \le C/N^{l+\lambda'-1/2}$ with $\lambda' < \lambda$.

The constant c depends on f, l, λ'.

The Approximation of True Solutions

Given μ_N an approximate solution of (2.7), define the approximate solution u_N of (2.1) using the integral of (2.4).

$$u_N(A) = \int_S \mu_N(q) \left(\frac{e^{ikr_{qA}}}{4\pi r_{qA}} + \chi(A,q) \right) d\sigma_q, \qquad A \in D_+. \tag{5.7}$$

To show the convergence of $u_N(A)$, we need the following lemma.

LEMMA 5.3.

$$\sup_{A \in K} \int_S \left| \frac{e^{ikr_{qA}}}{4\pi r_{qA}} + \chi(A,q) \right| d\sigma_q < \infty, \qquad \text{where } K \text{ is any compact subset of } D_+. \tag{5.8}$$

PROOF. From [4], $\sup_{A \in \Re^3} \int_S |e^{ikr_{qA}}/4\pi r_{qA}|\, d\sigma_q < \infty$.

Then

$$\sup_{A \in K} \int_S \left| \frac{e^{ikr_{qA}}}{4\pi r_{qA}} \right| d\sigma_q < \infty. \tag{5.9}$$

Furthermore, as $\chi(A,q)$ is continuous, $\int_S |\chi(A,q)|\, d\sigma_q$ is a continuous function in A. Therefore, we can conclude that $\sup_{A \in K} \int_S |\chi(A,q)|\, d\sigma_q < \infty$.

Combining this result with (5.9) proves (5.8). ∎

In practicality, for any bounded set of points in D_+, we can find a compact set K to enclose all of the given points. So this condition is sufficient to ensure convergence.

Since $u(A) - u_N(A) = \int_S (\mu(q) - \mu_N(q))(e^{ikr_{qA}}/4\pi r_{qA} + \chi(A,q))\, d\sigma_q$ it follows from Lemma 5.3 that

$$|u(A) - u_N(A)| \le c \|\mu - \mu_N\|_\infty, \qquad A \in D_+,$$

for some constant c. Thus, the convergence of μ_N leads to the convergence of $u_N(A)$ to $u(A)$, for all $A \in D_+$.

REMARK. Since $\chi(A,q)$ is a solution to the Helmholtz equation for each fixed q, satisfying the Sommerfeld radiation condition, $|\chi(A,q)| < c_q/|A|$ (for more details, see [6]). c_q depends on q. Therefore,

$$\sup_{A \in \Re^3 \setminus B} \int_S |\chi(A,q)|\, d\sigma_q \le \sup_{A \in \Re^3 \setminus B} \int_S \frac{c_q}{|A|}\, d\sigma_q,$$

where B is a ball of radius R and center at the origin such that $\bar{B}$ is a subset of a domain D_- containing the origin. If c_q is integrable on S, then we can prove that

$$\sup_{A \in \Re^3 \setminus B} \int_S |\chi(A,q)|\, d\sigma_q < \infty.$$

Combining this result with the fact that

$$\sup A \in \Re^3 \setminus B \int_S \left| \frac{e^{ikr_{qA}}}{4\pi r_{qA}} \right| d\sigma_q < \infty$$

(see [14]), we obtain

$$\sup_{A\in\Re^3\setminus B}\int_S\left|\frac{e^{ikr_{qA}}}{4\pi r_{qA}}+\chi(A,q)\right|d\sigma_q<\infty.$$

We have not ascertained this fact as yet. ∎

6. IMPLEMENTATION OF GALERKIN'S METHOD

Most of the work of this method is in the setup of the linear system (5.5) and in the evaluation of u_N. And in both cases, the most costly step is the numerical integration of surface integrals,

$$I(f)=\int_U f(q)d\sigma_q=\int_0^{2\pi}\int_0^{\pi}f(\phi,\theta)\sin\theta\,d\theta\,d\phi \text{ over } U. \tag{6.1}$$

The integral is approximated by

$$I_M(f)=\frac{\pi}{M}\sum_{i=1}^{2M}\sum_{j=1}^{M}w_j f\left(\phi_i,\theta_j\right) \tag{6.2}$$

or

$$\tilde{I}_M(f)=\frac{\pi}{M}\sum_{i=1}^{2M}\sum_{j=1}^{M}\tilde{w}_j f\left(\phi_i,\tilde{\theta}_j\right),\qquad M\geq 1. \tag{6.3}$$

Here $\phi_j=j\pi/M$, and $\{w_j\}$, $\{\cos\theta_j\}$ are the Gauss-Legendre weights and nodes on $[-1,1]$. $\{\tilde{w}_j\}$, $\{\tilde{\theta}_j\}$ are chosen from an idea of Iri, Moriguti and Takasawa [15]. (For an English explanation of this paper see [16].) There a change of variable to $[-1,1]$ has been used. The integral for $u_N(A)$ is evaluated using (6.2).

Calculation of the Galerkin Coefficients

Coefficients $(\hat{K}h_j,h_i)$ are fourfold integrals with a singular integrand. Since K is singular, the "inner integral" $\hat{K}h_j$ is a singular integral and must be evaluated with care. Since $\hat{K}h_j$ is itself a very smooth function, the inner product, which we call the "outer integral", is an integration involving a smooth integrand, thus only small number of node points are needed. To calculate $\hat{K}h_j$, we first rotate the surface S such that $\hat{p}$ is not a singular point internal to the integration region $[0,\pi]\times[0,2\pi]$ (for details see [17]). Then, we use (6.3) to evaluate the integral for $\hat{K}h_j$. The integral for $(\hat{K}h_j,h_i)$ is evaluated using (6.2). Because the Galerkin coefficients $(\hat{K}h_j,h_i)$ depend only on the surface S, we calculate them separately, say for $N\leq N_{\max}$, and they are stored in a disk, in a form for rapid retrieval by the main program used in solving (2.1). To decrease the effect of the singularity in computing $\hat{K}h_j(\hat{p})$, as in [13,18], we use the identity

$$\int_S-\frac{\partial}{\partial\nu_q}\frac{1}{r_{qp}}\,d\sigma_q=2\pi,\qquad p\in S$$

to write

$$\hat{K}h_j(\hat{p})=2\pi h_j(\hat{p})+\int_U\left[h_j(\hat{q})\widehat{\frac{-\partial}{\partial\nu_p}\frac{1}{r_{qp}}}+h_j(\hat{p})\widehat{\frac{\partial}{\partial\nu_q}\frac{1}{r_{qp}}}\right]|J(\hat{q})|\,d\sigma_{\hat{q}}$$
$$+\int_U h_j(\hat{q})\frac{-\partial}{\partial\nu_p}\left[\widehat{\frac{e^{ikr_{qp}}-1}{r_{qp}}}+4\pi\chi(p,q)\right]|J(\hat{q})|\,d\sigma_{\hat{q}},$$

where $J(\hat{q})$ is the Jacobian.

7. NUMERICAL EXAMPLES

In this section, several numerical examples are presented. The true solutions are given by

$$u_1(x,y,z) = \frac{e^{ikr}}{r},$$
$$u_2(x,y,z) = \frac{e^{ikr}}{r^2}\left(1+\frac{i}{kr}\right)z,$$
$$u_3(x,y,z) = \frac{e^{ikr}}{r^3}\left(-1+\frac{3}{k^2r^2}-\frac{3i}{kr}\right).0.5\left(3z^2-r^2\right), \qquad \text{where } r=\sqrt{x^2+y^2+z^2}.$$

Let NINTI denote M in (6.3) for calculating $\hat{K}h_j$ and NINTE denote M in (6.2) for calculating $(\hat{K}h_j, h_i)$. Let NINT denote M in (6.2) for calculating u_N. For convenience, we chose NINT = NINTI in all numerical examples. Let NDEG denote the degree of the approximate spherical harmonics; recall that the number d of basis functions equals to $(\text{NDEG}+1)^2$. These notations will be the same as that given in the program. We use NINTI = 16 or 32, NINTE = 8, 16, or 20. For the sphere in most cases (unless otherwise stated) only five terms were used from the series χ (for more details see p. 59). According to Jones [3] this is sufficient to remove the first five interior Dirichlet eigenvalues and obtain unique solutions at the same time. The graphing was done using spherical coordinates for the sphere and the heart shape and rectangular coordinates for the ellipsoid. We used double precisions for all calculations in ALPHA 2100 (5/300 Mhz) and FORTRAN programming language was used for the programming.

EXAMPLE 1. Let $S = U$.

Table 1. $k = 1$, NDEG = 7, NINTI = 16, NINTE = 16, true solution u_1.

Approximate Solution			
Point	Real Part	Imaginary Part	Absolute Error
(10,11,12)	5.06455257110D − 02	1.3224589887D − 02	1.271D − 06
(5,6,7)	−4.6337650093D − 02	−8.3331722564D − 02	2.332D − 06
(1,2,3)	−2.2057584538D − 01	−1.5092507584D − 01	6.588D − 06
(1,1,1)	−9.2699606870D − 02	5.69874051260D − 01	1.413D − 05

Table 2. $k = 1$, NDEG = 7, NINTI = 16, NINTE = 16, true solution u_1.

Approximate Solution			
Point	Real Part	Imaginary Part	Absolute Error
(10,11,12)	5.06435739910D − 02	1.32241333150D − 02	7.355D − 07
(5,6,7)	−4.6335873120D − 02	−8.3328510899D − 02	1.338D − 06
(1,2,3)	−2.2056745315D − 01	−1.5091923292D − 01	3.658D − 06
(1,1,1)	−9.2695992570D − 02	5.69852376440D − 01	7.843D − 06

For the numerical results in Table 1, I used coefficient (2.8), given by Kleinman and Roach. But for the rest of the tables, I used coefficient (2.9) which does not satisfy Theorem 2.1, but gives better results (see Table 2). According to Kleinman and Kress [19], coefficient (2.9) ensures not only unique solvability for the sphere and the perturbation of the sphere, but also minimizes the norm of the modified integral operator and minimizes the condition number of the integral equations.

Next, we added 13 terms from the series χ, and obtained Table 3a.

As we can see from Table 3a, the results are slightly worse than those in Table 2. Therefore, we increased the number of integration nodes, and obtained the results in Table 3b.

We can see from Table 3b, that when you increase the integration nodes, the accuracy is even better than in Table 2, where only five terms from the series were added. Thus, we can add more

Table 3a. $k = 1$, NDEG = 7, NINTI = 16, NINTE = 16, true solution u_1.

Approximate Solution			
Point	Real Part	Imaginary Part	Absolute Error
(10,11,12)	5.0642870802D − 02	1.3223948823D − 02	1.461D − 06
(5,6,7)	−4.6335231402D − 02	−8.3327348851D − 02	2.666D − 06
(1,2,3)	−2.2056440208D − 01	−1.5091707109D − 01	7.397D − 06
(1,1,1)	−9.2694692400D − 02	5.6984448934D − 01	1.584D − 05

Table 3b. $k = 1$, NDEG = 7, NINTI = 32, NINTE = 16, true solution u_1.

Approximate Solution			
Point	Real Part	Imaginary Part	Absolute Error
(10,11,12)	5.0644259117D − 02	1.3224312346D − 02	6.481D − 08
(5,6,7)	−4.6336499690D − 02	−8.3329639249D − 02	4.889D − 0
(1,2,3)	−2.2057043477D − 01	−1.5092128914D − 01	4.191D − 08
(1,1,1)	−9.2697244834D − 02	5.6986008141D − 01	1.173D − 07

Table 4. $k = 2$, NDEG = 7, NINTI = 16, NINTE = 8, true solution u_2.

Approximate Solution			
Point	Real Part	Imaginary Part	Absolute Error
(10,11,12)	2.82585146760D − 02	1.68239679910D − 02	4.410D − 07
(5,6,7)	−3.6153903844D − 02	5.24555285290D − 02	8.115D − 07
(1,2,3)	5.09312359600D − 02	2.10102657320D − 01	2.824D − 06
(1,1,1)	−2.8564591616D − 01	−1.9691057580D − 01	4.332D − 06

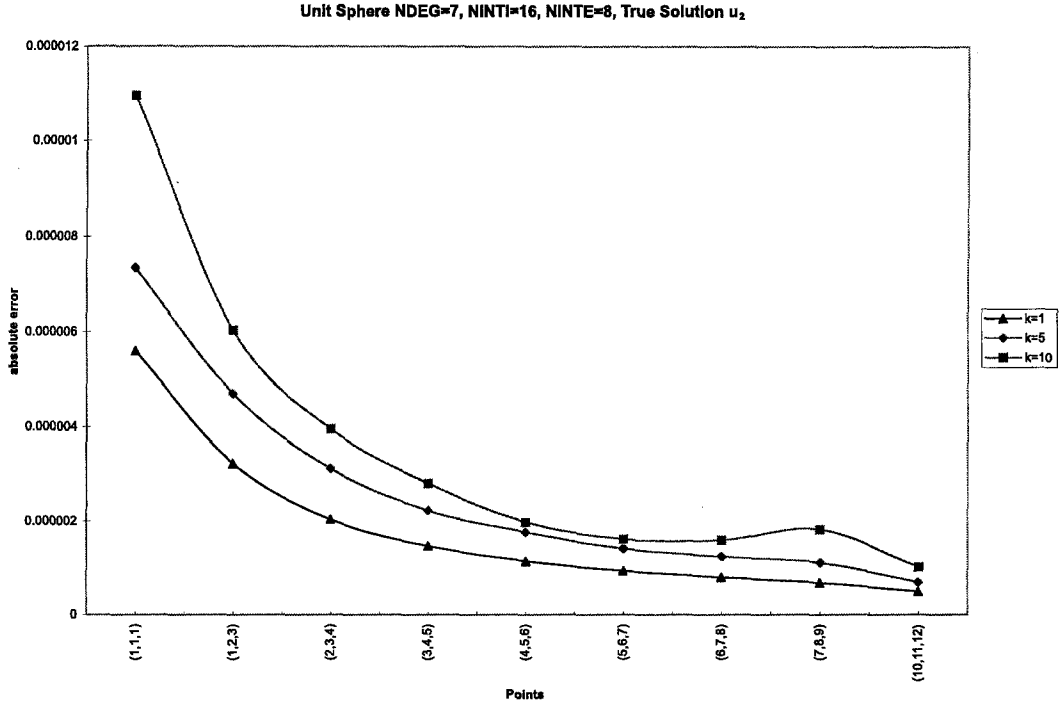

Figure 1. The further the points are from the boundary, the smaller the error.

than five terms and still obtain good results if we increase the number of integration nodes. But as more terms and increasing use of integration nodes increases the CPU time considerably, we decided to use only a few terms, only five for other cases of the sphere.

Table 5. $k = 15$, NDEG = 7, NINTI = 32, NINTE = 20, true solution u_1.

Approximate Solution			
Point	Real Part	Imaginary Part	Absolute Error
(10,11,12)	−4.0379358010D − 02	−3.3303789817D − 02	8.729D − 07
(5,6,7)	9.25751582790D − 02	2.28211922320D − 02	3.436D − 07
(1,2,3)	2.43616937720D − 01	−1.0990695838D − 01	3.383D − 07
(1,1,1)	3.81899030130D − 01	4.32996984690D − 01	1.160D − 07

From Tables 3a, 3b, and 4, we see that for the points away from the boundary there is much greater accuracy than for points near the boundary, which is shown in Figure 1. This is because the integrand is more singular at points near the boundary. Now, we look at the case of $k = 15$, given in Table 5. We first used NINTI = 16 in calculating the Galerkin coefficients $(\hat{K}h_j, h_i)$, the accuracy was not that good. Then, we changed NINTI to 32, the approximate solutions are printed and errors are printed in the column absolute error.

From Table 5, we see that to obtain similar accuracy as in the tables before, we need to increase the integration nodes. This is due to the following fact: the kernel function involves $\sin kr$ and $\cos kr$, and these trigonometric functions are much more oscillatory when k becomes large. In this case, we must increase the integration nodes to achieve the same accuracy. From the column of absolute errors, we see that the accuracy is similar to the previous tables.

REMARK. We picked NINTE < NINTI, because the integrand of $(h_i, \hat{K}h_j)$ is smoother than the integrand of $\hat{K}h_j$. We also pick NINTE $\geq$ (NDEG + 1). Now let us pick $k = 10.904122$, an eigenvalue of the interior Dirichlet problem, and represent the solution as a single layer potential in Table 6a and as a modified single layer potential in Table 6b.

As we can see from the above tables, the accuracy in Table 6a is quite poor as expected, compared to Table 6b.

The eigenvalues were computed from the following equation:

$$J_n(kr) = 0.$$

For more details on how to obtain the eigenvalues for the sphere see [1,20,21].

Table 7 illustrates the effects on the error for different integration nodes for fixed N = NDEG. (Note: when NINTI = 8, NINTE = 8, we denote it as 8,8.)

Table 6a. $k = 10.904122$, NDEG = 7, NINTI = 16, NINTE = 8, true solution u_2.

Approximate Solution			
Point	Real Part	Imaginary Part	Absolute Error
(10,11,12)	−1.8670079230D − 04	−8.6010197177D − 05	3.301D − 02
(5,6,7)	−1.7201975199D − 04	−2.2529585848D − 04	6.390D − 02
(1,2,3)	8.90108837010D − 04	−3.4750527588D − 04	2.152D − 01
(1,1,1)	−1.3905775038D − 03	5.12590981200D − 04	3.351D − 01

Table 6b. $k = 10.904122$, NDEG = 7, NINTI = 16, NINTE = 8, true solution u_2.

Approximate Solution			
Point	Real Part	Imaginary Part	Absolute Error
(10,11,12)	1.82451007840D − 02	2.7352339373D − 02	4.071D − 06
(5,6,7)	1.85705241690D − 02	6.0873017910D − 02	7.991D − 06
(1,2,3)	−2.1433276896D − 01	3.6050529843D − 03	2.649D − 05
(1,1,1)	3.32478364930D − 01	2.9914089411D − 02	4.077D − 05

Table 7. Unit sphere, $k = 10$, NDEG $= 7$, true solution u_2.

Absolute Error			
Point	8,8	16,8	32,8
(10,11,12)	5.948D − 06	4.810D − 07	6.504D − 09
(5,6,7)	1.153D − 05	9.309D − 07	8.819D − 09
(1,2,3)	3.987D − 05	3.213D − 06	2.186D − 08
(1,1,1)	1.682D − 03	3.017D − 05	4.301D − 08

EXAMPLE 2. Now, we look at the following "heart-shaped" surface given by

$$x = \left(A - \frac{\epsilon}{1+\alpha(\cos\theta+1)^2}\right)\cos\phi\sin\theta,$$
$$y = \left(A - \frac{\epsilon}{1+\alpha(\cos\theta+1)^2}\right)\sin\phi\sin\theta,$$
$$z = \left(A - \frac{\epsilon}{1+\alpha(\cos\theta+1)^2}\right)\cos\theta.$$

For the numerical examples, we choose $A = 2$ and 3, $\epsilon = 0.0005$ and 1 and $\alpha = 90,000$. Coefficient (2.9) was used with $O(\epsilon) = 0$. For more details, see [8,18]. For the perturbation of the sphere examples, only four terms from the series were added. Let S the perturbation of the sphere given by $A = 2$ and $\epsilon = 1$.

Table 8. $k = 3$, NDEG $= 7$, NINTI $= 16$, NINTE $= 8$, true solution u_1, $\epsilon = 0.0005$, $A = 3$, $\alpha = 90000$.

Approximate Solution			
Point	Real Part	Imaginary Part	Absolute Error
(10,11,12)	3.7711007793D − 02	3.6297891589D − 02	2.946D − 06
(8,9,10)	−6.3003944242D − 02	1.0582346035D − 02	3.543D − 06
(5,6,7)	9.5231525793D − 02	4.6106057671D − 03	4.827D − 06
(4,5,6)	4.2122297328D − 02	1.0588552142D − 01	5.329D − 06

Now, we added ten terms from the series, and obtained similar results. When we increased the integration nodes to NINTI $= 16$, NINTE $= 16$, the accuracy was similar to NINTI $= 16$, NINTE $= 8$. But when we increased the integration nodes to NINTI $= 32$, NINTE $= 16$, the accuracy was worse. This is because $O(\epsilon)$ depends on k, A, and ϵ, so the number of terms added from the series effects the value of it. So, when we increased the terms from five to ten, $O(\epsilon)$ should have changed accordingly. As we used the same $O(\epsilon) = 0$, the accuracy does not improve when you increase the nodes. Therefore, we decided to add only a few terms, only four in the case of the perturbation of the sphere with $O(\epsilon) = 0$.

REMARK. For each case, we changed either one or two or all the variables, A, ϵ, α and the wave number k. As shown in Figure 2, also in this case, further the points are away from the boundary greater the accuracy.

Table 9. $k = 0.2$, NDEG $= 7$, NINTI $= 16$, NINTE $= 8$, true solution u_1, $\epsilon = 1$, $A = 2$, $\alpha = 90000$.

Approximate Solution			
Point	Real Part	Imaginary Part	Absolute Error
(13,14,15)	5.8958879932D − 03	−4.0746267190D − 02	7.798D − 05
(11,12,13)	−2.4999930131D − 02	−4.0981781458D − 02	9.142D − 05
(5,6,7)	−4.7797213032D − 02	8.2546435026D − 02	1.911D − 04
(4,5,6)	−2.0662211419D − 02	1.1213656803D − 01	2.346D − 04

Table 10. $k = 3$, NDEG $= 7$, NINTI $= 16$, NINTE $= 8$, true solution u_2, $\epsilon = 0.0005$, $A = 3$, $\alpha = 90000$.

Approximate Solution			
Point	Real Part	Imaginary Part	Absolute Error
(10,11,12)	2.3290276491D − 02	2.3210713205D − 02	6.060D − 07
(8,9,10)	−4.0395476188D − 02	5.9062317657D − 03	7.819D − 07
(5,6,7)	6.3463463135D − 02	5.0944668600D − 03	1.022D − 06
(4,5,6)	2.6054700078D − 02	7.3495501007D − 02	1.323D − 06

Table 11. $k = 7$, NDEG $= 7$, NINTI $= 32$, NINTE $= 16$, true solution u_1, $\epsilon = 0.0005$, $A = 3$, $\alpha = 90000$.

Approximate Solution			
Point	Real Part	Imaginary Part	Absolute Error
(13,14,15)	3.8187488655D − 02	1.5405021498D − 02	8.409D − 06
(12,13,14)	2.9338872470D − 02	3.3236983709D − 02	9.583D − 06
(6,7,8)	−6.6536183870D − 02	−4.7810466238D − 02	1.795D − 05
(5,6,7)	−3.8060446955D − 02	−8.7425043115D − 02	1.993D − 05

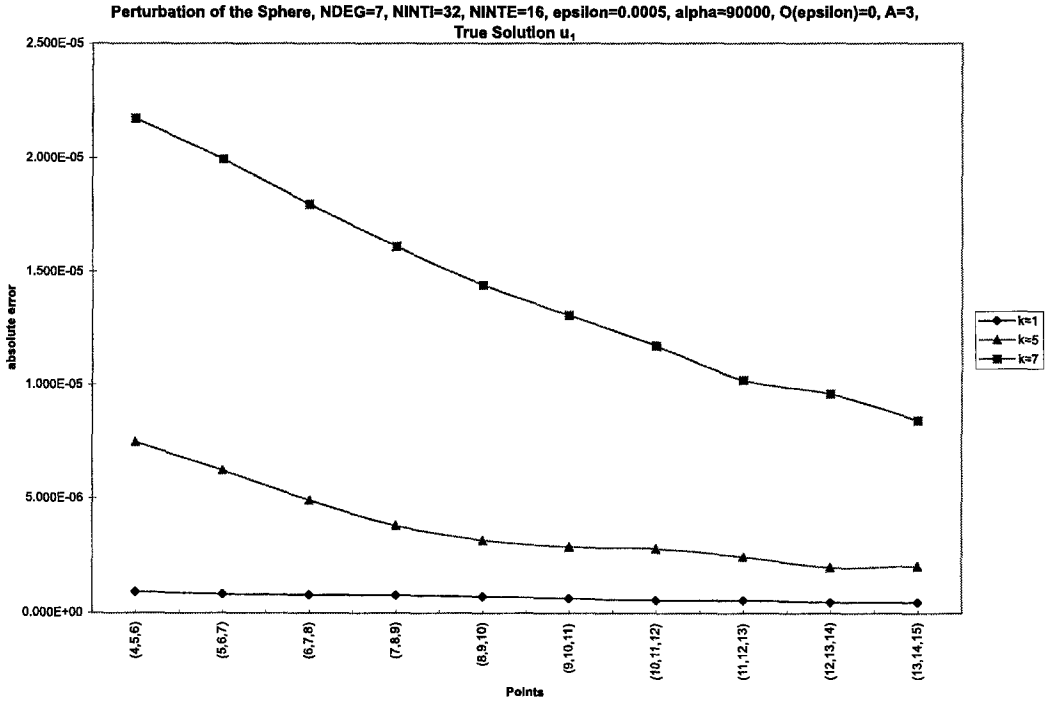

Figure 2. The further the points are from the boundary, the smaller the error.

Table 12. $k = 1$, NDEG $= 7$, NINTI $= 32$, NINTE $= 20$, true solution u_1.

Approximate Solution			
Point	Real Part	Imaginary Part	Absolute Error
(10,11,12)	5.06012000140D − 02	1.31451931860D − 02	9.005D − 05
(5,6,7)	−4.6395940078D − 02	−8.3178312668D − 02	1.626D − 04
(1,2,3)	−2.2063954680D − 01	−1.5054443375D − 01	3.832D − 04
(1,1,1)	−9.2005918423D − 02	5.69158666690D − 01	9.849D − 04

Table 13. $k = 1$, NDEG = 7, NINTI = 32, NINTE = 20, true solution u_2.

Approximate Solution			
Point	Real Part	Imaginary Part	Absolute Error
(10,11,12)	3.1144936626D − 02	9.6722626389D − 03	3.775D − 04
(5,6,7)	−2.5761775603D − 02	−5.7838650473D − 02	7.393D − 04
(1,2,3)	−1.4424829446D − 01	−1.6564909847D − 01	2.635D − 03
(1,1,1)	−2.3888747606D − 01	2.9712649578D − 01	4.689D − 03

Table 14. $k = 1$, NDEG = 7, NINTI = 16, NINTE = 16, true solution u_1.

Approximate Solution			
Point	Real Part	Imaginary Part	Absolute Error
(10,11,12)	5.06425966970D − 02	1.32236483650D − 02	1.808D − 06
(5,6,7)	−4.6335212291D − 02	−8.3326699099D − 02	3.258D − 06
(1,2,3)	−2.2056355497D − 01	−1.5091585111D − 01	8.807D − 06
(1,1,1)	−9.2686264839D − 02	5.69841801700D − 01	2.140D − 05

Table 15. $k = 2$, NDEG = 7, NINTI = 32, NINTE = 16, true solution u_1.

Approximate Solution			
Point	Real Part	Imaginary Part	Absolute Error
(10,11,12)	4.5642258569D − 02	2.5569438092D − 02	2.765D − 05
(5,6,7)	−5.0272040505D − 02	8.0962334706D − 02	4.817D − 05
(1,2,3)	9.6772055376D − 02	2.4898591855D − 01	1.308D − 04
(1,1,1)	−5.4731950047D − 01	−1.8284122382D − 01	3.032D − 04

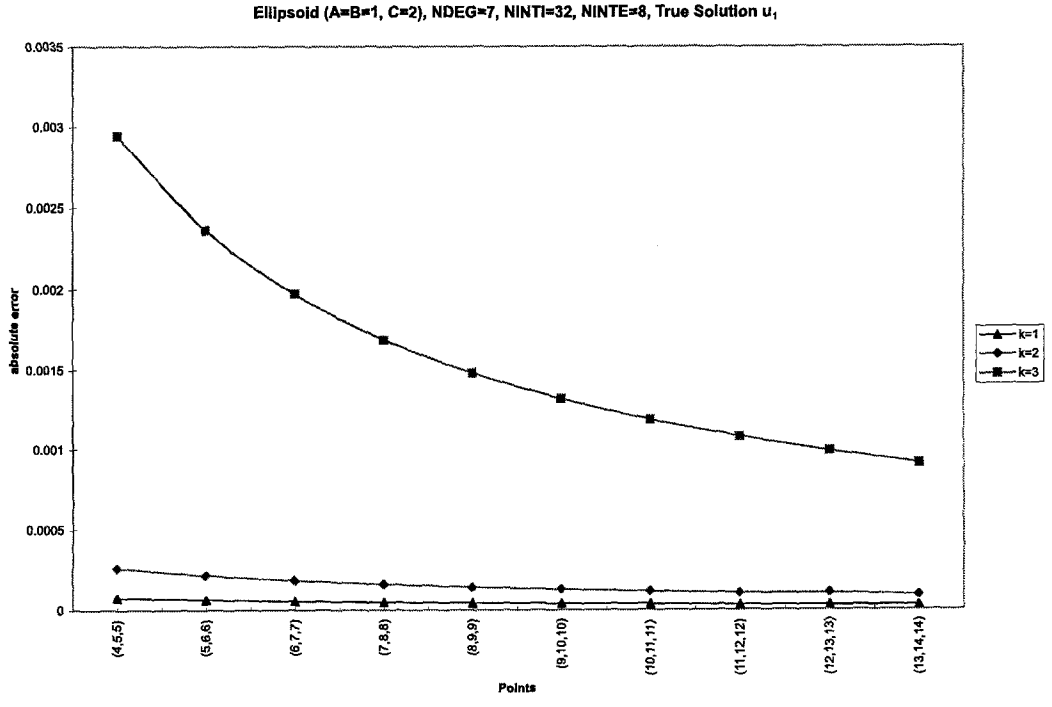

Figure 3. The further the points are from the boundary, the smaller the error.

Now, we look ellipsoids of revolution around the z axis. There are no explicit coefficient choices for the ellipsoids. Furthermore the coefficient for the sphere does not work well for the ellipsoids, thus the following coefficient choice was made by numerical experimentation.

EXAMPLE 3. Let S be the ellipsoid surface $x^2+y^2+(z/2)^2=1$. For this case, we choose $R=\gamma\rho$. Here $\rho=\sqrt{x^2+y^2+z^2}$ and $\gamma=$ the average of the eccentricities of the three cross section ellipses that the ellipsoid is made of. So we chose $R=\gamma\sqrt{1+3(\cos\theta)^2}$ for the first example. For all the numerical examples only five terms from the series were added.

Now, we look at another example of a similar ellipsoid for two different wave numbers.

EXAMPLE 4. $x^2+y^2+(z/1.5)^2=1$. Here $R=\gamma\sqrt{1+1.25(\cos\theta)^2}$.

Also in this case there is better accuracy for points away from the boundary as shown in Figure 3.

Comments

In all of our experiments, we only added a few terms from the series. This is because in numerical calculations it is inefficient to add the full series. So we allow only a small number of coefficients a_{nm} to be different from zero.

According to Jones [3], this is sufficient to ensure uniqueness for the modified integral equations in a finite range of wave numbers k. In practical applications, one is usually concerned with a finite range of k so this is not a serious draw back. For the case of the ellipsoid, when you increase the k, you get reasonable results, but we need a large amount of nodes to get good results. In order to use a large amount of nodes, we need a considerably high amount of CPU time. For all calculations, we used ALPHA 2100 (5/300 Mhz). The programs for the Bessel functions were taken from NSWC library of mathematics subroutines.

From the above examples, we see that the error is effected by the boundary S, NINTI, NINTE, boundary data, and k.

The role of k is more significant for ill-behaved boundary shapes. If we want to obtain more accuracy, we must increase the number of integration nodes for calculating the Galerkin coefficients $(\hat{K}h_j, h_i)$. Here, we give some idea of the cost of calculating the Galerkin coefficients. When NINTI or NINTE are doubled, the CPU time increases about four times (see Table 18).

Table 16. NDEG = 7, $k=5$, five terms from the series were added.

NINTI,NINTE	CPU Time (minutes)
16,8	5:15
16,16	21:34
32,16	83:00

Some of the increased cost comes from the complex number calculations, which is an intrinsic property of the Helmholtz equation. Furthermore any integration method is affected by k, due to the oscillatory behavior of the fundamental solution e^{ikr}/r. Also the CPU time depends on the number of terms added from the series. Calling subroutines from NSWC may have increased the CPU time further (see Table 19).

As we see from the Table 19, the more terms you add the larger the CPU time, thus in order to remove a higher number of interior Neumann eigenvalues, we need a more powerful computer.

Table 17. NINTI = 32, NINTE = 16, NDEG = 7, $k=5$.

Number of Terms For The Series	CPU Time (hours)
5	1:23
10	4:37
13	7:25

REMARK. ALPHA 2100 (5/300 Mhz) computer system allows us to add up to 28 terms from the series, with NINTI = 32, NINTE = 8. After 28 terms the system cannot handle the computation of the Bessel functions, and gives a floating overflow error. Furthermore, though we can add

28 terms with NINTI = 32, NINTE = 8, the accuracy is not very good. Thus in order to obtain accurate results, for example similar to five terms from the series, we need to increase the integration nodes. For this purpose, as mentioned above, we need a more powerful computer system.

8. THE ACCURACY OF THE GALERKIN COEFFICIENTS ON THE UNIT SPHERE

In here, we obtain the true Galerkin coefficients (Kh_j, h_i) explicitly on the unit sphere, and compare it with the approximate Galerkin coefficients. This will give us an idea of the accuracy of the Galerkin coefficients which are effected by k and the integration nodes. Let $q \in$ the unit sphere, with center at O and A is outside the unit sphere. From [21], we have for $|A| > 1$,

$$\frac{e^{ikr}}{4\pi r} = ik \sum_{n=0}^{\infty} (2n+1) j_n(k) h_n^{(1)}(k\,|A|) p_n(\cos\theta), \tag{8.1}$$

where $r = |A - q|$, θ is the angle formed by OA and Oq, and $j_n(z)$ and $h_n^{(1)}(z)$ are spherical Bessel and Hankel functions. That is

$$j_n(z) = \frac{\sqrt{\pi}}{2} \left(\frac{z}{2}\right)^{-1/2} J_{n+1/2}(z),$$
$$h_n^{(1)}(z) = \frac{\sqrt{\pi}}{2} \left(\frac{z}{2}\right)^{-1/2} H_{n+1/2}^{(1)}(z).$$

For the definitions of $J_{n+1/2}$, $H_{n+1/2}$ and related definitions see Section 2. To be consistent with (8.1), we rewrite the series $\chi(A, q)$ in the following form:

$$\chi(A, q) = ik \sum_{n=0}^{\infty} a_{nm} (2n+1) h_n^{(1)}(k\,|A|)\, h_n^{(1)}(k) p_n(\cos\theta), \tag{8.2}$$

where a_{nm} is coefficient (2.9) given in the previous sections. From (8.1) and (8.2)

$$K\mu(A) = \int_S \frac{\partial}{\partial q} ik \sum_{n=0}^{\infty} (2n+1) h_n^{(1)}(k\,|A|) \left(j_n(k) + a_{nm} h_n^{(1)}(k)\right) \mu(q) p_n(\cos\theta)\, d\sigma_q,$$

where K is defined as in the first section. Thus, following the same argument as [7,22], we can obtain

$$K\mu(p) = \left[-2\pi i k^2 \left(j_n'(k) h_n(k) + j_n(k) h_n'(k)\right) + 2\pi i k^2 a_{nm} h_n^{(1)}(k) h_n^{(1)'}(k)\right] \mu(p), \tag{8.3}$$

where $p \in S$ (when A coincides with p which is the intersection of OA and the circle). Let h_i, h_j be any two basis functions of spherical harmonics (see previous section). From (8.3)

$$\frac{(Kh_i, h_i)}{(h_i, h_i)} = \left[-2\pi i k^2 \left(j_n'(k) h_n(k) + j_n(k) h_n'(k)\right) + 2\pi i k^2 a_{nm} h_n^{(1)}(k) h_n^{(1)'}(k)\right], \tag{8.4}$$

where

$$h_i = \left\{ \begin{array}{c} p_n(\cos\theta), \\ p_n^m(\cos\theta) \begin{bmatrix} \cos m\phi \\ \sin m\phi \end{bmatrix}, \quad m = 0, \ldots, n. \end{array} \right\}$$

And note that $(Kh_j, h_i) = 0$, for all i and j. This also can be derived from the fact that $K = 0$ on the sphere with a_{nm} chosen as in (2.9) (see [18]). Thus, the matrix formed by the Galerkin coefficients is a zero matrix on the sphere (see (8.4)).

Let NINTI and NINTE be defined as in the previous section. The errors are printed in Table 18.

Table 18. $k = 1$, error for the Galerkin coefficients on the unit sphere.

NINTI,NINTE	$\deg h_i = 0$	$\deg h_i = 1$	$\deg h_i = 2$
8,4	4.0162949D − 03	5.33689177D − 16	3.91754193D − 15
32,4	2.780836828D − 06	1.349255679D − 09	6.526628377D − 09

From Table 18, we see that if the integration nodes are increased, the accuracy is much improved for $\deg h_i = 0$. For $k = 10$, we have similar accuracy. For $\deg h_i = 1$ and $\deg h_i = 2$, the accuracy is good at 8,4: thus, when you increase the nodes, the rounding errors come into play and the results were slightly worse.

From Table 19, we see that the accuracy of the Galerkin coefficients for NINTI = 16 is poor for $\deg h_i = 0$ case. But for NINTI = 32, the accuracy is better for $\deg h_i = 0$.

Table 19. $k = 15$, Error for the Galerkin coefficients on the unit sphere.

NINTI,NINTE	$\deg h_i = 0$	$\deg h_i = 1$	$\deg h_i = 2$
16,4	1.260187315D − 01	3.15368378D − 13	2.3897378D − 12
32,4	2.639917601D − 06	1.349253663D − 09	6.52665421D − 09

REFERENCES

1. H.A. Schenk, Improved integral formulation for acoustic radiation problems, *Journal of the Acoustical Society of America*, 41–58, (1967).
2. A.J. Burton and G.F. Miller, The application of integral equation methods to the numerical solution of some exterior boundary-value problems, *Proc. Roy. Soc. London, A* **323**, 201–210, (1971).
3. D.S. Jones, Integral equations for the exterior acoustic problem, *Q. J. Mech. Appl. Math.* **27**, 129–142, (1974).
4. T.C. Lin, The numerical solution of the Helmholtz equation using integral equations, Ph.D. Thesis, University of Iowa, Iowa City, IA, (July 1982).
5. D. Colton, *Partial Differential Equations*, (1988).
6. D. Colton and R. Kress, *Integral Equation Methods in Scattering Theory*, (1983).
7. R.E. Kleinman and G.F. Roach, On modified Green functions in exterior problems for the Helmholtz equation, *Proc. R. Soc. Lond. A* **383**, 313–333, (1982).
8. R.E. Kleinman and G.F. Roach, Operators of minimal norm via modified Green's functions, *Proceedings of the Royal Society of Edinburgh* **94A**, 163–178, (1983).
9. T.C. Lin, Smoothness results of single and double layer solutions of the Helmholtz equations, *Journal of Integral Equations and Applications* **1** (1), 83–121, (1988).
10. T.M. Macrobert, *Spherical Harmonics*, Third Edition, Pergamon Press, New York, (1967).
11. K.E. Atkinson, The numerical solution of the Laplace's equation in three dimensions, *SIAM J. Numer. Anal.* **19**, 263–274, (1982).
12. D. Ragozin, Constructive polynomial approximation on spheres and projective spaces, *Trans. Amer. Math. Soc.* **162**, 157–170, (1971).
13. K.E. Atkinson, ALGORITHM 629, An integral equation program for Laplace's equation in three dimensions, *ACM Transactions on Mathematical Software* **11** (2), 85–96, (June 1985).
14. T.C. Lin, The numerical solution of Helmholtz equation for the exterior Dirichlet problem in three dimensions, *SIAM, J. Numerical Anal.* **22** (4), 670–686, (1985).
15. M. Iri, S. Moriguti and Y. Takasawa, On a numerical integration formula (in Japanese) Research Inst. for Math. Sciences, Kyoto University, Volume 91, p. 82, (1970).
16. K.E. Atkinson, Numerical integration on the sphere, *J. Austral. Math. Soc., Series B* **23**, 332–347, (1982).
17. K.E. Atkinson, *The Numerical Solution of Integral Equations of the Second Kind*, Cambridge University Press, (1998).
18. K.E. Atkinson, The numerical solution of Laplace's equation in three dimensions-II, In *Numerical Treatment of Integral Equations*, (Edited by J. Albrecht and L. Collatz) pp. 1–23, Birkhauser Verlag, Base, (1980).
19. R.E. Kleinman and R. Kress, On the condition number of integral equations in acoustics using modified fundamental solutions, *IMA Journal of Applied Mathematics* **31**, 79–90, (1983).
20. A.J. Burton, The solution of Helmholtz' equation in exterior domains using integral equations, Division of Numerical Analysis and Computing, Teddington, Middlesex, NPL Report NAC 30, (1973).
21. M. Abramovitz and I. Stegun, Editors, *Handbook of Mathematical Functions*, National Bureau of Standards, Washington D.C., (1964).
22. W. Magnus, F. Oberhettinger and K.P. Soni, *Formulas and Theorems for the Special Functions of Mathematical Physics*, Springer, New York, (1966).
23. J.F. Ahner and R.E. Kleinman, The exterior Neumann problem for the Helmholtz equation, *Arch. Rational Mech. Anal.* **52**, 26–43, (1973).
24. K.E. Atkinson, *In Introduction to Numerical Analysis*, John Wiley, New York, (1978).
25. T.C. Lin, A proof for the Burton and Miller integral equation approach for the Helmholtz equation, *Journal of Mathematical Analysis and Applications* **103** (2), 565–574, (1984).
26. O.I. Panich, On the question of the solvability of the exterior boundary problem for the wave equation and the Maxwell's equation (In Russian), *Uspekhi. Mat. Nauk.* **20**, 221–226, (1965).
27. F. Ursell, On the exterior problems of acoustics, II, *Proc. Cambridge Phil. Soc.* **84**, 545–548, (1978).